Energy gaps in graphene nanomeshes

William Oswald and Zhigang Wu[*]

Department of Physics, Colorado School of Mines, Golden, Colorado 80401, USA
(Received 24 December 2011; revised manuscript received 8 March 2012; published 22 March 2012)

We report on the band gap opening and electronic structures of graphene nanomeshes (GNMs), the defected graphene containing a high-density array of nanoscale holes, from first-principles calculations. As expected, quantum confinement at the GNM necks leads to a sizable band gap; however, surprisingly, the appearance of a gap depends sensitively on the hole arrangement and periodicity. For the simplest hexagonal zigzag-edged holes passivated by hydrogen, two-thirds of GNMs remain semimetallic while the rest are semiconductors. Furthermore, we show that the energy gap opening in GNM results from the combination of quantum confinement and the periodic perturbation potential due to perforation.

I. INTRODUCTION

Graphene, a two-dimensional (2D) single-layer honeycomb structure of carbon (C), has stimulated tremendous research interests due to its many amazing properties including extremely high mobility (exceeding $15\,000$ cm^2/Vs),[1,2] making it an excellent candidate to replace silicon in electronics and optoelectronics.[3] However, its zero band gap (E_g) semimetallic behavior must be adjusted to allow a meaningful on-off ratio in graphene-based field-effect transistors (FETs). A number of approaches have been proposed to tune the band gap in graphene, including graphene nanoribbons (GNRs),[4–6] Stone-Thrower-Wales (STW) and inverse-Stone-Thrower-Wales (ISTW) types of defects,[7–10] boron and nitrogen doping,[11,12] hydrogen passivation,[13] etc. However, currently these methods are limited either in technological capability or in scalability.

Recently, extensive investigations[14–24] have been carried out on constructing periodic nanoscale holes on graphene, known as the graphene nanomesh (GNM). Experimentally, Bai *et al.*[17] used block copolymer lithography to prepare GNM with various periodicities and hole diameters, and they showed that GNM-based FETs had on-off ratios similar to those of GNR devices, indicating a sizable band gap. Most importantly, GNM devices are able to carry electric currents about 100 times greater than a single GNR. Furthermore, the band gap in GNM can be tuned by varying the neck width, the shortest distance between two neighboring holes. Akhavan[18] produced GNMs using the local photodegradation of graphene oxide sheets at the top of ZnO nanorods, demonstrating the *p*-type semiconducting properties without doping. Thus GNM could allow for large-scale fabrication of the long-sought graphene-based electronics and optoelectronics; however, facilitating rational design requires elucidating the mechanisms leading to band gap opening and evaluating the quantitative relationship between E_g and the structural parameters of GNM from fundamental theory.

Enormous efforts have been made on theoretical models and calculations on GNMs to predict the change in electronic structures due to lattice modification by perforating.[14–16,19–24] Since a GNM is a geometrically defected single hexagonal sheet of C atoms, its electronic behaviors could be described by the simple tight-binding (TB) approximation with the single-parameter nearest-neighbor π-orbital model. For instance,

Pedersen *et al.*[14] found a scaling rule for E_g with respect to the numbers of removed and original total C atoms in a unit cell. However, first-principles computations based on the density functional theory (DFT) have revealed much richer electronic structures and predicted the subtle band gap opening due to individual set of structural parameters of a GNM, though the scaling rule for E_g agrees in general with that derived from simple arguments. For instance, Ouyang *et al.*[24] predicted half of GNMs were semimetals and the rest were semiconductors, while Şahin and Ciraci[21] pointed out that only one-third of their calculated GNMs had significant nonzero band gaps. Previous theoretical works have not sufficiently considered GNMs systematically or thoroughly analyzed the band-opening mechanism.

In this article, we carry out DFT computations to show that only one-third of GNMs with hydrogen passivation and the zigzag-edged hexagonal holes are semiconductors, whose band gaps satisfy the scaling rule discovered previously. The appearance of an energy gap in these GNM systems with zigzag-edged holes is comparable to that in GNRs with armchair edges, in the sense that both the quantum confinement and the edge effects play crucial roles. However, for the rectangular hole arrangement we have studied, increasing the distance between neighboring holes along the zigzag lattice direction causes the GNM to vary from semimetal to semiconductor with a periodicity of 3, while along the armchair direction it only changes the magnitude of E_g if it is a semiconductor. In contrast to armchair GNRs and C nanotubes (CNTs),[25] two-thirds of which have substantial band gaps, whereas only one-third are semiconductors. This can be understood from the complementary structures of GNMs and GNRs, and the modified symmetry and periodicity of GNMs relative to graphene also play crucial roles in energy gap opening, in addition to quantum confinement.

II. METHODS

We employ the self-consistent pseudopotential calculations using both the plane-wave basis (implemented in the VASP package[26,27]) and the linear combination of atomic orbital (LCAO) basis (implemented in the SIESTA package[28]), with the Perdew-Burke-Ernzerhof (PBE)[29] parametrization of the generalized gradient approximation (GGA). We only use
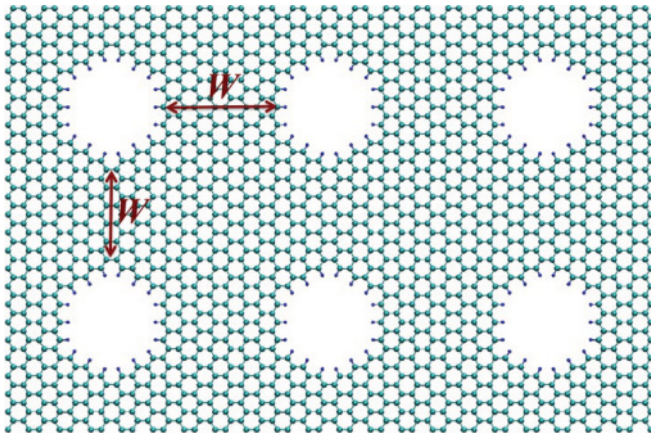
FIG. 1. (Color online) A typical H-passivated GNM system. Here the big cyan (small blue) spheres represent C (H) atoms, and W denotes the neck width along the zigzag and armchair directions.

the VASP package to check the accuracy of the SIESTA computations; specifically, the band structure of graphene has been well reproduced using an optimized double-ζ plus polarization (DZP) basis set with an energy cutoff of 300 Ry for the real space mesh. We fully relax all the GNMs until the maximum atomic force is less than 0.02 eV/Å, using a $2 \times 2 \times 1$ **k** mesh which leads to good convergence for the large unit cells. All the calculations are spin polarized, and the antiferromagnetic state is found to have the lowest energy for the systems considered here, in agreement with previous works.[15,22,23] We have checked the effects of vacuum spacing, and the 4-nm spacing is found to be well converged since further increasing it makes no change in all results.

The systems studied in this work have the rectangular unit cell, as shown in Fig. 1, where the edges of holes are passivated with hydrogen atoms. We focus on the simple hexagonal holes with zigzag edges, which are realistic experimentally, to explore the essential physics and fundamental mechanisms responsible for the change of electronic structures of graphene due to the occurrence of holes. The results for more complicated cases of hole shape and arrangement will be reported elsewhere.[30] The lattice constants of rectangular unit cells range from about 1 to 5 nm, with the hole diameter varying from 3.6 to 20.6 Å. The neck widths (W, as shown in Fig. 1) are the difference between lattice constants and the hole diameter, which indicate the strength of quantum confinement.

As illustrated in Fig. 2, we classify the unit cells of these GNMs by the numbers (P and Q) of the repeating conventional

cells for the perfect graphene along the armchair (x) and zigzag (y) directions, respectively, and the x axis is parallel to one zigzag hole edge. Thus, we refer to a GNM studied in this work with lattice parameters P and Q as ($P \times Q$) GNM; for example, those in panels (a)–(c) of Fig. 2 are named as (6×7), (6×8), and (6×9) GNM, respectively. Then we put the information of the hole in parentheses, such as (6×9) GNM ($d = 7.8$ Å), as shown in Fig. 2(c). This hexagonal hole corresponds to 24 C atoms removed from a unit cell.

III. RESULTS

As plotted in Fig. 3, band structures of GNMs have almost symmetrical near-gap valence and conduction bands with respect to the Fermi energy level (defined as the medium point of band gap in a semiconductor). This is derived from the behavior of π orbitals in graphene; if only the nearest-neighbor interaction is considered,[3] the occupied and unoccupied bands are symmetrical. Our electronic structure calculations reveal two distinct types of band structures of these GNMs, as summarized in Fig. 3, where the figures in panels (a), (b), and (c) correspond to the band structures of GNMs illustrated in panels (a), (b), and (c) in Fig. 2, respectively. The band structures plotted in Figs. 3(a) and 3(b) look very similar, representing a semimetal with a zero (or nearly zero) band gap close to the K point within the 2D Brillouin zone (BZ), while Fig. 3(c) indicates that the associated GNM is a semiconductor with a direct band gap at the Γ point. Other GNMs computed have band structures similar to one of these three, depending on their lattice parameters P and Q.

GNMs depicted in Figs. 2(a), 2(b), and 2(c) have $P = 6$ and $Q = 7$, 8, and 9, respectively. We find that if the hole remains the same, increasing P only reduces E_g gradually without affecting the characteristics of the band structure, while varying Q leads to variation between semimetallic and semiconducting behaviors. As shown in Fig. 4(a), when $Q = 3m + 1$ or $3m + 2$ (where m is a positive integer), GNMs are a zero-gap (or almost zero gap) semimetal, with band structures very similar to those plotted in Fig. 3(a) or 3(b), respectively, whereas for $Q = 3m$, GNMs are semiconductors, whose band structures are nearly identical to that plotted in Fig. 3(c).

Figure 4(a) shows that for the semiconducting family with a fixed hole, E_g as a function of lattice parameters P and Q
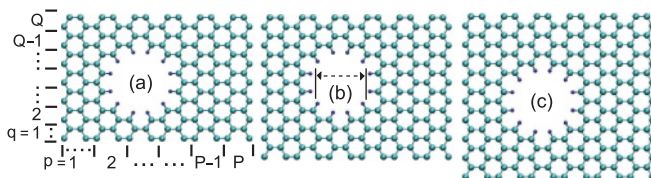

FIG. 2. (Color online) Unit cells for three GNMs. Here P and Q indicate the periodicity along the x and y axes, respectively, and the hole has a diameter [as indicated in panel (b)] of 7.8 Å for all three cases. In these three GNMs, $P = 6$, while (a) $Q = 7$, (b) $Q = 8$, and (c) $Q = 9$.
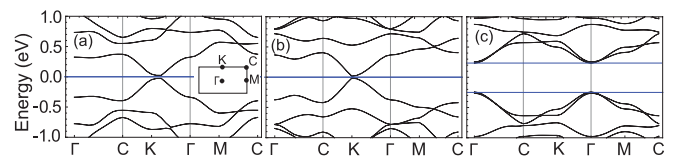

FIG. 3. (Color online) Electronic band structures of three GNMs, which are shown in Figs. 2(a), 2(b), and 2(c), respectively. The inset in panel (a) illustrates the first Brillouin zone of a GNM with the rectangular unit cell. The horizontal blue (gray) lines indicate the energy levels of the Fermi energy in panels (a) and (b) and the valence band maximum and conduction band minimum in panel (c).
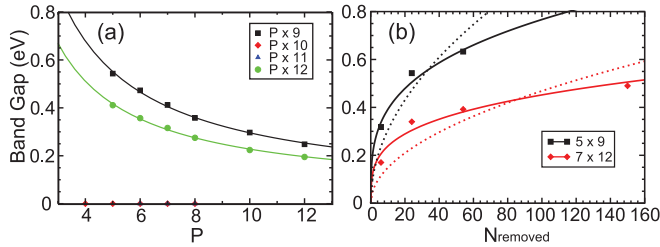
FIG. 4. (Color online) Band gap (E_g) as a function of structural parameters of GNMs. (a) E_g dependence of lattice parameters P and Q [as defined in Fig. 2(a)] for a fixed hole, and (b) E_g dependence of hole size for fixed lattice parameters. The solid and dotted curves are fitted to the calculated data points (see text for details).

well satisfies the formula proposed by Pedersen *et al*.:[14]

$$E_g = g \frac{N_{removed}^{1/2}}{N_{total}}, \qquad (1)$$

where g is a constant obtained from fitting numerical data, and $N_{removed}$ and N_{total} are the numbers of removed and total (before removing C atoms to make meshes) C atoms in a unit cell, respectively. This scaling rule was derived from simple arguments for any semiconductor sheets. In Fig. 4(a), each curve corresponds to fixed values of $N_{removed}$ and Q; as a result, $N_{total} \propto P$ and $E_g \propto 1/P$. The fitted values of g for $Q = 9$ and 12 are 19 and 16 eV, respectively, comparable with $g = 25$ eV fitted by Pedersen *et al*. for their calculated TB results. For other values of Q (10 and 11), g is very close to zero and GNMs are semimetallic.

On the other hand, Fig. 4(b) plots E_g scaling with hole size for fixed lattice parameters. Here the Pederson scaling (the dotted lines) fits only qualitatively, and we modify it to get better fitting:

$$E_g = g \frac{N_{removed}^{\alpha}}{N_{total}}, \qquad (2)$$

where α is the scaling exponent. In this case, N_{total} is fixed and $E_g \propto N_{removed}^{\alpha}$. Fitting to the ($5 \times 9$) and ($7 \times 12$) GNMs [the solid lines in Fig. 4(b)] gives $\alpha \approx 0.3$, while $g = 35$ and 42 eV, respectively. Therefore, our DFT calculations suggest that the scaling of E_g in GNMs with respect to $N_{removed}$ and N_{total} are more complex than originally proposed, depending on the way the structure expands. For only varying the hole size, $E_g \propto N_{removed}^{0.3}/N_{total}$, indicating that small holes punctuated on graphene would open a gap greater than previously predicted.

The dependence of E_g on GNM structures, as summarized in Fig. 4, clearly demonstrates the important role that the quantum confinement plays in band gap opening. Quantum confinement manifests itself in GNMs by the neck widths; in either case of fixing hole size while changing lattices or fixing lattices while changing hole size, W measures the strength of quantum confinement, leading to the variation in E_g when $Q = 3m$. Actually, the scaling of $E_g \propto 1/P$ for fixed hole size means $E_g \propto 1/(W + \text{constant})$, exactly the same as that predicted in GNRs.[4]

The most interesting finding in this work is that the ($P \times 3m + i$) GNMs belong to one of the *three* families depending upon $i = 0$, 1, or 2; within each family they have comparable electronic properties. This interesting behavior

has been predicted previously in armchair GNRs, in which there are three families as well, classified by the width of nanoribbon.[4] It is also well known that CNTs have three families, determined by their chirality numbers (n, m).[25] However, in contrast to CNTs and armchair GNRs, among which two-thirds are semiconductors and one-third are semimetallic (or having very small gap in armchair GNRs), only one-third of these GNMs we have studied are semiconductors, whereas the rest are semimetals. The similar family-of-3 type of gap opening-closing behaviors have been predicted in GNMs[21] with very different settings than ours, and qualitatively it could be understood from the antidot nature of GNMs.

IV. DISCUSSION

Fundamental understanding of the gap opening in GNMs could be gained using the TB model of the π bond with the nearest-neighbor interaction. However, GNMs have very large 2D unit cells with hundreds to thousands of C atoms and complex boundary conditions at hole edges; thus, a direct analysis based on an analytical Hamiltonian is extremely difficult. The essential physics involved, however, is that the periodic perturbation due to periodic holes modifies the band structure of pristine graphene, tuning its gapless Dirac point to open up a gap.

For the vicinity of the Dirac point (K in the BZ of graphene, as shown in Fig. 5), a small wave vector $\mathbf{q}$ is defined as $\mathbf{q} + \mathbf{K} = \mathbf{k}$, and the famous linear energy dispersion of graphene is given as

$$E_{\pm}(\mathbf{q}) = E_0 \pm \hbar v_F q, \qquad (3)$$

where the Fermi speed $v_F = 840$ km/s, by solving the free-particle Shrödinger equation

$$v^2 q^2 \Psi(x, y) = E^2 \Psi(x, y). \qquad (4)$$

The introduction of periodic holes in graphene could be modeled as perturbative infinite potential, causing wave functions $\Psi(x, y)$ to disappear at the hole edge. With this hard-wall boundary condition, the energy dispersion is changed,
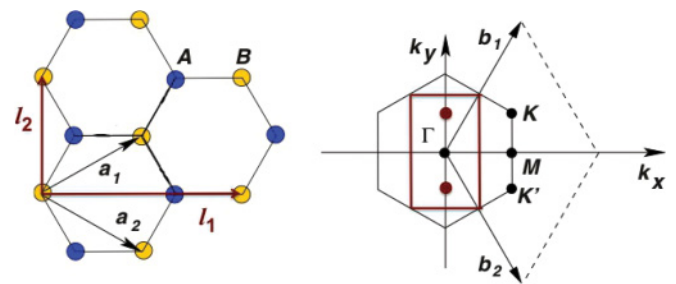

FIG. 5. (Color online) Graphene lattice and its first Brillouin zone. On the left is the honeycomb structure with the A and B sublattices. $\mathbf{a}_1$ and $\mathbf{a}_2$ are the lattice vectors for the primitive unit cell (two atom per cell), while $\mathbf{l}_1$ and $\mathbf{l}_2$ are the lattice vectors for the conventional rectangular unit cell (four atom per cell). On the right are the corresponding Brillouin zones. The black hexagonal one is for the primitive cell, while the dark red (gray) rectangular one corresponds to the conventional cell. The two dark red (gray) points inside the conventional cell indicate the Dirac points.

becoming smooth rather than singular around the Dirac point, similar to those for GNRs and CNTs.

In the (primitive) hexagonal BZ of graphene, there are six Dirac points, and all of them are folded to the k_y axis in the BZ for the four-atom (conventional) rectangular unit cell, as shown in Fig. 5. For a GNM with the $P \times Q$ rectangular unit cell (as shown in Fig. 2), the **k** points in the BZ for the four-atom unit cell are further folded $P - 1$ and $Q - 1$ times into its BZ along k_x and k_y axes, respectively. Therefore, along the Γ-K direction of GNM's BZ [see the inset of Fig. 3(a)] exists the original Dirac point, where the band gap opening might occur. In total, there are $2PQ - N_{\text{removed}}/2$ occupied and unoccupied π bands, nearly symmetrical with respect to the Fermi energy level. Many of these bands derive directly from pristine graphene without noticeable changes, except for those close to the Fermi energy, where the hard-wall boundary condition at hole edges causes energy dispersion different from Eq. (4) since the eigenvalues $E_\pm(\mathbf{k})$ based on the TB model for pristine graphene cannot well describe these bands anymore. This is in sharp difference from CNTs and GNRs, where the band gap opening originates from quantized wave vectors **k** along the confined direction,[31–33] so that the original gap closing conditions for $E_\pm(\mathbf{k})$ might not be satisfied. Varying Q in a GNM changes the energy dispersion characteristics along the critical Γ-K direction, while changing P only gradually modifies the dispersion quantitatively.

The boundary conditions of GNMs and GNRs are different in that GNMs still have the 2D continuity, while GNRs only have 1D; hence, their gap-opening mechanisms are distinctive as well. Nevertheless, the essential effect of quantum confinement due to GNM's necks is expected to be similar to that in GNRs caused by ribbon width, as evidenced by the facts that increasing neck width of a semiconductor GNM reduces the band gap and that the scaling of E_g is very similar to that of GNRs. Thus, a GNM can be simply approximated as parallel GNRs with width the same as GNM's neck width, with the hard-wall boundary condition on GNM's hole edges extended to the lines perpendicular to its necks. Along the x axis, these parallel GNRs are of the armchair type, while along y axis they are of the zigzag type. *Ab initio* calculations[4] have shown that there are three families of armchair GNRs, all of which have energy gaps. However, one family has much smaller gap than the other two for similar width, and within the nearest-neighbor TB approximation this family is semimetallic. On the other hand, the zigzag GNRs have only one family: semiconductors with relatively smaller gaps. Based on these previous results of GNRs, this simple model is consistent with the observation that only varying Q can change a GNM from a semimetal to a semiconductor; but only one-third of GNMs are semiconductors since GNMs have much less quantum confinement compared with GNRs with the same width as GNM's neck width.

Graphene consists of A and B sublattices (Fig. 5). In this study, the hexagonal holes perforated have the same number of A-type (n_A) and B-type (n_B) C atoms; therefore, these GNMs systems keep the global balance of $n_A = n_B$. However, the hexagonal holes have zigzag edges, which break the local balance of these two sublattices and which might lead to localized states (flat electronic bands). We find these flat bands (not shown in band structures as in Fig. 3) in these systems have

much lower energies than Fermi energy, and consequently, they do not affect the gap opening or change the magnitude of the gap. However, they appear in other systems with more complex hole edges.

V. CONCLUSIONS

We have also performed systematical studies of a wide range of other GNM systems with different periodic arrangements and with a large variety of hole shapes and edges, not just what have been reported here. Our essential finding is qualitatively consistent with other GNM systems, though there is ample and sometimes subtle dependence of electronic structures on geometry. These results will be reported elsewhere.[30] Since our conclusions were drawn not based on certain GNM structures, and the mechanism involved can be elucidated from fundamental physics principles, our calculations indicate that the specific hole sizes and arrangements do not play a critical role on the basic relationship between band gap and geometry. The method of patterning holes to tune band gap can be readily applied to other nanoscale structures, such as carbon nanotubes (CNTs), where the metallic CNTs might be made semiconducting so that the great difficulty in separating them from other intrinsically semiconducting CNTs could be overcome. Furthermore, theoretically, our finding suggests that although quantum confinement is important in band gap opening and tuning the size of gap, other structural factors and in particular, nanoscale patterning, could also play a critical role, providing additional strategies for controlling electronic and optoelectronic behaviors of nanoscale materials.

In summary, we conclude that the band-gap-opening mechanism in GNMs is different from that in GNRs, although quantum confinement plays a crucial role in both systems. The periodic perturbation induced by periodic nanoscale holes causes a GNM to change between a semimetal and a semiconductor, depending upon the variation of lattice vectors. Though the gap opening in GNMs could be understood qualitatively from comparing with GNRs that have comparable widths with GNM's neck widths, the 2D structure of GNMs leads to a much higher proportion of metallic systems than that in 1D GNRs and CNTs. The complexity of GNMs reveals an ample and subtle relationship between structure and properties, and the combination of quantum confinement at hole edges and the modified symmetry and periodicity due to hole arrangement leads to interesting and unexpected phenomena. Thus, our study points to a venue for manipulating materials at the nanoscale for desirable properties.

*zhiwu@mines.edu

[1] K. S. Novoselov, A. K. Geim, S. V. Morosov, D. Jiang, Y. Zhang, S. B. Dubonos, I. V. Grigorieva, and A. A. Firsov, Science **306**, 666 (2004).

[2] A. K. Geim and K. S. Novoselov, Nat. Mater. **6**, 183 (2007).

[3] A. H. C. Neto, F. Guinea, N. M. R. Peres, K. S. Novoselov, and A. K. Geim, Rev. Mod. Phys. **81**, 109 (2009).

[4] Y. W. Son, M. L. Cohen, and S. G. Louie, Phys. Rev. Lett. **97**, 216803 (2006).

[5] Y. W. Son, M. L. Cohen, and S. G. Louie, Nature (London) **444**, 347 (2006).

[6] V. Barone, O. Hod, and G. E. Scuseria, Nano Lett. **6**, 2748 (2006).

[7] P. A. Thrower, in *Chemistry and Physics of Carbon*, edited by P. L. Walker Jr. (Dekker, New York, 1969), Vol. 5, p. 262.

[8] A. Stone and D. Wales, Chem. Phys. Lett. **128**, 501 (1986).

[9] M. T. Lusk and L. D. Carr, Phys. Rev. Lett. **100**, 175503 (2008).

[10] M. T. Lusk, D. T. Wu, and L. D. Carr, Phys. Rev. B **81**, 155444 (2010).

[11] L. Ci, L. Song, C. Jin, D. Jariwala, D. Wu, Y. Li, A. Srivastava, Z. F. Wang, K. Storr, L. Balicas, F. Liu, and P. M. Ajayan, Nat. Mater. **9**, 430 (2010).

[12] L. S. Panchakarla, K. S. Subrahmanyam, S. K. Saha, A. Govindaraj, H. R. Krishnamurthy, U. V. Waghmare, and C. N. R. Rao, Adv. Mater. **21**, 4726 (2009).

[13] J. O. Sofo, A. S. Chaudhari, and G. D. Barber, Phys. Rev. B **75**, 153401 (2007).

[14] T. G. Pedersen, C. Flindt, J. Pedersen, N. A. Mortensen, A.-P. Jauho, and K. Pedersen, Phys. Rev. Lett. **100**, 136804 (2008).

[15] W. Liu, Z. F. Wang, Q. W. Shi, J. Yang, and F. Liu, Phys. Rev. B **80**, 233405 (2009).

[16] K. Lopata, R. Thorpe, S. Pistinner, X. Duan, and D. Neuhauser, Chem. Phys. Lett. **498**, 334 (2010).

[17] J. Bai, X. Zhong, S. Jiang, Y. Huang, and X. Duane, Nat. Nanotech. **5**, 190 (2010).

[18] O. Akhavan, ACS Nano **4**, 4174 (2010).

[19] H. Jippo, M. Ohfuchi, and C. Kaneta, Phys. Rev. B **84**, 075467 (2011).

[20] R. Petersen, T. G. Pedersen, and A. P. Jauho, ACS Nano **5**, 523 (2011).

[21] H. Şahin and S. Ciraci, Phys. Rev. B **84**, 035452 (2011).

[22] X. Y. Cui, R. K. Zheng, Z. W. Liu, L. Li, B. Delley, C. Stampfl, and S. P. Ringer, Phys. Rev. B **84**, 125410 (2011).

[23] H. Yang, M. Chshiev, X. Waintal, and S. Roche (unpublished).

[24] F. Ouyang, S. Peng, Z. Liu, and Z. Liu, ACS Nano **5**, 4023 (2011).

[25] J.-C. Charlier, X. Blase, and S. Roche, Rev. Mod. Phys. **79**, 677 (2007).

[26] G. Kresse and J. Hafner, Phys. Rev. B **48**, 13115 (1993).

[27] G. Kresse and J. Furthmüller, Phys. Rev. B **54**, 11169 (1996).

[28] J. M. Soler, E. Artacho, J. D. Gale, A. Garca, J. Junquera, P. Ordejn, and D. Snchez-Portal, J. Phys.: Condens. Matter **14**, 2745 (2002).

[29] J. P. Perdew, K. Burke, and M. Ernzerhof, Phys. Rev. Lett. **77**, 3865 (1996).

[30] W. Oswald and Z. Wu (in preparation).

[31] K. Wakabayashi, M. Fujita, H. Ajiki, and M. Sigrist, Phys. Rev. B **59**, 8271 (1999).

[32] M. Ezawa, Phys. Rev. B **73**, 045432 (2006).

[33] H. Zheng, Z. F. Wang, Tao Luo, Q. W. Shi, and J. Chen, Phys. Rev. B **75**, 165414 (2007).